On the Response of Short Ocean Wave Components at a Fixed Wavenumber to Ocean Current Variations

O. M. PHILLIPS

Department of Earth & Planetary Sciences, Johns Hopkins University, Baltimore, MD 21218

(Manuscript received 10 November 1983, in final form 26 March 1984)

ABSTRACT

This paper is concerned with the patterns in the degree of saturation of short wind-generated waves (at scales much smaller than those of the spectral peak but large compared with the capillary scales) that are produced by current variations in the presence of wind energy input and loss by breaking or by the formation of parasitic capillaries. It has two aims: the first is to provide a base for interpretation of patterns observed in synthetic aperture radar imagery in terms of current features. The second is to give analytical expressions for the magnitude of the variations in degree of saturation produced by given current fields so that, when appropriate quantitative measurements become available, better parametric representations of the energy loss rates can be developed.

Particular care is taken to provide physically based representations of wind input and loss by wave breaking and a relatively convenient equation (4.2) is derived that specifies the distribution of the degree of saturation in a current field, relative to its ambient (undisturbed) background in the absence of currents. The magnitude of the variations in b depends on two parameters, U_0/c, where U_0 is the velocity scale of the current and c the phase speed of the surface waves at the (fixed) wavenumber considered or sampled by SAR, and $S = (L/\lambda)(u_*/c)^2$, where L is the length scale of the current distribution, λ the wavelength of the surface waves and u_* the friction velocity of the wind. When S is large (of order 10 or more) the distribution of b is insensitive to currents for which $U_0/c \sim 1$, but when S is of order unity or less, significant variations in b are produced. A convergence zone is associated with a maximum in b relative to its ambient levels of

$$b_{\max} = \left\{1 + \frac{9}{4\pi m}\frac{U_0}{cS}\right\}^{11/(n-1)},$$

where $m \approx 0.04$ and $n \sim 3$. This appears as a bright line in the SAR imagery against the ambient background. In general, changes of order unity in b (and the return SAR signal) should be observed if the local current strain-rate scale

$$U_0/L \gtrsim 0.12 g^{-1/2}\lambda^{-3/2}u_*^2 .$$

A local divergence or upwelling reduces the relative degree of saturation; when S is small the reduction is by the factor $(1 + 2U/c)^{-9/2}$ and continues until the waves grow back to the equilibrium level under the influence of the wind. A divergence line would be imaged as a line across which the return decreases relatively abruptly from the ambient level upwind, to a lower level downwind, gradually recovering to the ambient.

1. Introduction

The variety of instruments now available for active radio probing of the ocean surface makes possible the observation over a wide area of oceanic features ranging from capillary and microscale breaking waves to long ocean swells. Variations in the return signal with position on the ocean surface gives indications of even large scale features such as mesoscale ocean eddies and the distribution of surface wind stress. The scales of the surface features responsible for the return signal depend upon the wavelength of the incident radiation. When the angle of incidence on the water surface is not close to normal and the wavelength of the radiation is large compared with the scales of occasional local occurrences such as breaking waves, the return signal seems, as a result of careful measurements such as those of Keller and Wright (1975), to be the result of first-order Bragg scattering from predominantly freely traveling surface waves. The wavenumber k of the surface wave sensed is

$$k = 2k_i \sin\theta, \tag{1.1}$$

where k_i is the wavenumber of the incident radiation and θ the angle of incidence; the depression angle is $\frac{1}{2}\pi - \theta$. A real or synthetic aperture radar (SAR) at a frequency of 1.5 GHz responds to a surface wavelength of the order of 10 cm at a depression angle of 30° or so, and a high-resolution image such as that from SAR gives, in the pattern of intensity variations in the return signal, the pattern of local energy density of surface disturbances at this scale.

Some of these patterns are extremely intriguing. Beal *et al.* (1981) show a number of examples obtained from Seasat, a noteworthy one giving surface expressions of tidal flow over the Davis Shoals, southeast of Nantucket Island. Another, off the mouth of the Chesapeake Bay, suggests a complex pattern of eddies (or perhaps water masses); at high resolution the individual swell crests can be discerned. Fascinating as these images are, it is far from clear how they should be properly interpreted or what quantitative information they may contain. If we accept the premise that the images are derived primarily from freely traveling short gravity waves modified by longer waves and currents, then it should be possible to infer at least some properties of the current field, in particular, from the imagery. The short gravity waves sensed by the Seasat SAR do have a significant "lifetime" of propagation, unlike capillary waves which are transient and fugitive, and their interaction with longer waves and currents may significantly modify their distribution over the ocean surface. The object of this paper is to determine the extent to which this can occur and to seek relations by which quantitative information might be obtained from this imagery.

2. Action input and dissipation processes at short gravity-wave scales

Since we will be concerned with interactions between the short gravity waves and surface currents, the wave dynamics are specified most conveniently by the balance of action spectral density $N(\mathbf{k})$, which is related to the spectrum of surface displacement $\Psi(\mathbf{k})$ by

$$N(\mathbf{k}) = \frac{g}{\sigma}\Psi(\mathbf{k}) = (g/k)^{1/2}\Psi(\mathbf{k}), \tag{2.1}$$

where σ is the intrinsic frequency and $\Psi(k)$ is normalized such that the integral over the entire wavenumber plane

$$\int \Psi(\mathbf{k})d\mathbf{k} = \bar{\zeta}^2,$$

the mean square surface displacement. The spectral energy density of the wave field is $\rho g\Psi(\mathbf{k})$, where ρ is the water density.

Following energy paths, the balance of wave-action spectral density is given by

$$\frac{d}{dt}N(\mathbf{k}) = \frac{\partial N}{\partial t} + (\mathbf{C} + \mathbf{U})\cdot\nabla N$$
$$= -\nabla_k \cdot T(\mathbf{k}) + S_w - D, \tag{2.2}$$

(for example, see Phillips, 1980) where $\mathbf{C} = \nabla_k\sigma$ represents the group velocity and $\mathbf{U}$ the velocity of the surface current. The exchanges of action density among different wave components by wave–wave interactions are specified by the first term on the right, in which $\mathbf{T}(\mathbf{k})$ is the flux of action spectral density in the wavenumber plane. These interactions, in a gravity wave system, are conservative so that the integral over all $\mathbf{k}$ vanishes. The two remaining terms specify the spectral distribution of action input from the wind and the loss of action density (which at these scales is predominantly the result of sporadic wave breaking or possibly the formation of parasitic capillaries). Our present degree of understanding of the three processes represented on the right-hand side of (2.2) decreases monotonically in the order in which they are written though, as we shall see, some useful progress can be made.

The specification of the wave field is completed by use of the kinematical conservation equation

$$\frac{\partial \mathbf{k}}{\partial t} + \nabla(\sigma + \mathbf{k}\cdot\mathbf{U}) = 0 \tag{2.3}$$

together with the condition that $\nabla \times \mathbf{k} = 0$, and the dispersion relation giving the intrinsic frequency in terms of the wavenumber magnitude:

$$\sigma = (gk)^{1/2}. \tag{2.4}$$

If the underlying current is nonuniform, the wavenumber $\mathbf{k}$ of an energy packet varies as it propagates across the surface—$\mathbf{k} = \mathbf{k}(\mathbf{x}, t)$. On the other hand, in remote sensing by radar (such as the L-band SAR with a radar wavelength of 0.2 m), the Bragg scattering condition selects an almost fixed surface wavenumber $\mathbf{k}$ in (1.1), so that it is convenient in this context to rewrite (2.2) to refer to a fixed, rather than a variable wavenumber. From (2.3),

$$\frac{\partial k_i}{\partial t} = -\frac{\partial}{\partial x_i}(\sigma + k_j U_j)$$
$$= -\left(\frac{\partial \sigma}{\partial k_j}\frac{\partial k_j}{\partial x_i} + U_j\frac{\partial k_j}{\partial x_i} + k_j\frac{\partial U_j}{\partial x_i}\right),$$

but since $\nabla \times \mathbf{k} = 0$ and $C_j = \partial\sigma/k_j$,

$$\frac{dk_i}{dt} = \frac{\partial k_i}{\partial t} + (C_j + U_j)\frac{\partial k_i}{\partial x_j} = -k_j\frac{\partial U_j}{\partial x_i} \tag{2.5}$$

and since $N = N(\mathbf{k}, \mathbf{x}, t)$,

$$\frac{dN}{dt} = \frac{\partial N}{\partial t} + (C_j + U_j)\frac{\partial N}{\partial x_j} - k_j\frac{\partial U_i}{\partial x_j}\frac{\partial N}{\partial k_i}$$
$$= -\frac{\partial T_i}{\partial k_i} + S_w - D, \tag{2.6}$$

now for a fixed wavenumber $\mathbf{k}$.

To progress beyond this point, we need some assessment of the magnitude and nature of the terms represented schematically on the right of (2.2) or (2.6). The spectral energy and action transfers have been investigated extensively by Hasselmann and his co-workers, by West (1984) and by Fox (1976). There

is little doubt that resonant spectral-energy transfers influence significantly the components near the spectral peak and, as suggested by Kitaigorodskii (1983) over a range of higher frequencies up to those for which $c/u_* > 5$ at most. Just above the frequency of the spectral peak, the fractional rate at which action is acquired or lost by wave interactions per wave period in an active wave field is of the order 10^{-4} (Phillips, 1980) and this can be taken as an upper limit to the rate appropriate to smaller scales (0.1 to 1 m) of interest here. Even so, it is, as we shall see, generally less by about an order of magnitude than the rate at which action is acquired by short gravity waves from the wind, provided the wind is sufficient to produce any such components at all.

The energy transfer from wind to waves has been the subject of many theoretical and experimental enquiries during the past twenty-five years which have, if nothing else, demonstrated the complexity and variety of processes involved. At these small scales with wind blowing, the wave components are certainly of finite amplitude, with intermittently high curvature at their crests producing bursts of parasitic capillaries and occasional breaking. Air flow separation accompanies breaking as Banner and Melville (1976) have shown and Banner (1984) demonstrates that an enhanced local energy and momentum flux to the waves occurs as a result. Both the short waves and the wind are modulated and deflected by the longer waves and swell so that for the purposes of providing a more concrete expression for S_w in (2.2), the best guide is given by the results of careful measurements interpreted in the light of only very general theoretical considerations. Plant (1982), suggests from an examination of such measurements that

$$S_w(k) = 0.04\sigma\left(\frac{u_*}{c}\right)^2 \cos\theta N(k)$$

$$= m\sigma\left(\frac{u_*}{c}\right)^2 N(k), \quad \text{say} \qquad (2.7)$$

where u_* is the friction velocity, $c = (g/k)^{1/2}$, the phase speed of the component, and θ the angle between $\mathbf{k}$ and the wind. Plant estimates the numerical coefficient to be accurate to within ~50%. Mitsuyasu and Honda (1984) give a similar expression derived from their experiments, with a numerical coefficient of 0.07 but with no directional factor included. Phillips (1980) estimated a coefficient of 0.05 and Gent and Taylor's (1976) numerical calculations give approximately 0.07—the relatively small scatter of values obtained from independent calculations or sets of measurements gives some confidence that this is a reasonably accurate representation over the range $1 > u_*/c > 0.1$ that includes most short waves of interest. The specific directional factor ($\cos\theta$) suggested by Plant is less certain. Nevertheless, the base of data he used is both extensive and carefully evaluated, so that (2.7) can be adopted with reasonable confidence as a useful semi-empirical representation. Since we are principally concerned with short wave components with wavelengths of 10 cm or more and with wind speeds of order 10 m s^{-1} or less, the pertinent values of u_*/c do occupy the range specified above and the fractional rate at which action is acquired from the wind per wave period,

$$\frac{2\pi S_w(\mathbf{k})}{\sigma N(\mathbf{k})} \sim 0.3(u_*/c)^2 \cos\theta$$

ranges from 0.3 to 3×10^{-3} and is at least an order of magnitude larger than the net rate associated with wave–wave interactions.

If the wind-generated waves are superimposed on a variable current, the local rate of energy input to the waves will vary because of variations in the local wave-energy density and also possibly because of variations in the relative velocity of mean wind and current. In most cases of interest, the magnitudes of the current variations are small compared with the wind speed so that the influence of this latter effect is expected to be slight.

If the short wave components of the field have reached a state of statistical equilibrium in a region undisturbed by currents, then $dN(\mathbf{k})/dt = 0$ and since for these components $\nabla_k \cdot T$ is negligible, the densities of short wave breaking or parasitic capillaries must adjust themselves so that the dissipation D balances the wind input rate. Most previous observational studies on wave breaking, such as those of Toba and Kunishi (1970), have sought direct relationships between the density of whitecap coverage and wind stress. These implicitly assume such a statistical balance; our primary concern here is the response of the short wave structure when the balance is disturbed. Whether or not a particular wave crest breaks depends, in fact, on its configuration and time development and not directly on the wind speed, since (for example) breaking can be induced by a local adverse current, independent of the wind speed, and suppressed when the waves overtake a locally favorable current. Accordingly, D must be regarded intrinsically as a functional of the local spectral density, not the wind speed; its dependence on wind speed arises only insofar as this influences the spectral level or possibly, in the case of very short waves, as it influences the microscale breaking criterion through the surface drift (Phillips and Banner, 1974).

The spectral level is conveniently specified by the dimensionless function

$$B = g^{-1/2}k^{9/2}N(\mathbf{k}) = k^4\Psi(\mathbf{k}), \qquad (2.8)$$

which, in any particular spectrum, can be regarded as a function of $\mathbf{k}/k_0$, where k_0 is the wavenumber of the spectral peak. This function can be called "the degree of saturation." The simple idea of a saturation

range at high wavenumbers of the gravity wave spectrum (Phillips, 1958) assumed a hard upper limit B_s, independent of $\mathbf{k}/k_0$, for B (the saturation range "constant"), any further increase in the spectral level being prohibited by immediate wave breaking. Within the present conceptual framework, this corresponds to a dissipation function D that is negligibly small when $B < B_s$ but discontinuous (and in fact undefined) as $B \rightarrow B_s$. It is more realistic to assume that the action dissipation rate D 1) is a continuous function of the degree of saturation B that is zero when $B = 0$, 2) remains very small while B is significantly less than the old saturation range constant when breaking is rare, and 3) then increases rapidly when B approaches B_s and short wave breaking becomes denser in space and more frequent in time. Its form is then as indicated schematically in Fig. 1.

Also shown in Fig. 1 is the wind source term (2.7) which can now be written as

$$S_w(\mathbf{k}) = 0.04 \cos\theta(u_*/c)^2 g k^{-4} B(\mathbf{k}/k_0), \quad (2.9)$$

from (2.8). For a particular wavenumber this is linear in B to the accuracy of the expression (2.7) and the slope increases quadratically with u_*. The short waves are in statistical equilibrium at the degree of saturation B_0 defined by the intersection of these two curves. Note that, according to this description, the degree of saturation under equilibrium conditions may increase somewhat with wind speed, but the generally good observational support for the original idea of a "hard" saturation range indicates that the variation with wind speed must be weak and the curve of D as a function of B must increase very rapidly indeed. At the shorter gravity–capillary wavelengths to which a scatterometer is sensitive, the decay time and characteristic lifetimes of wave energy groups are much shorter than they are for gravity waves, so that the *average* degree of saturation over patches that are in some places highly saturated and in others, relatively unsaturated depends more strongly on wind speed than does the average degree of saturation of short gravity waves.

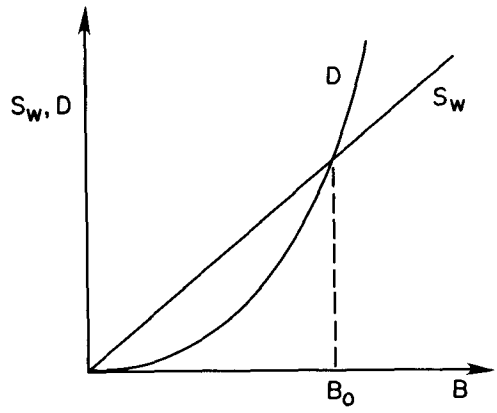

FIG. 1. Input from the wind S_w and dissipation D of action spectral density as functions of the degree of saturation B. The intersection specifies B_0, the high wavenumber equilibrium value.

Before our specification can be completed for the spectral density of action dissipation, there is one further conceptual difficulty that must be faced. Does the function D for a particular wavenumber depend on the degree of saturation at *that* wavenumber only or on its value over a range of surrounding (or perhaps distant) wavenumbers? An individual breaking event is localized in space within a distance probably of order k^{-1}; in Fourier space its influence is distributed over a range of wavenumbers of order k. Also, the statistics of wave breaking at a certain scale (defined by the phase speed of the breaking crest) cannot be expected in general to depend on the spectral density or the degree of saturation at that scale alone, but over a range of scales. Consequently the statistical characteristics of wave breaking and the dynamical consequences of breaking on the wave field both involve a possibly wide spectral range. However, if the degree of saturation B is almost constant over this range, a condition that might be anticipated under steady wind conditions, then on similarity grounds one might assert that

$$D = g k^{-4} f(B). \quad (2.10)$$

In situations in which a much longer swell is present, the degree of saturation of the short waves will vary with respect to phase of the swell, being greater near the crests (with local breaking) and much smaller in the troughs. Although an expression such as (2.10) may hold locally, the overall mean rate of action dissipation will depend not only on the mean degree of saturation but also on the swell slope, and this additional parameter should be included in (2.10).

The function $f(B)$ is illustrated only schematically in Fig. 1. Although its detailed form is not known at this stage, it may be possible to determine some of its characteristics more explicitly from laboratory or field observations. If the short waves are in a statistical balance between wind and dissipation, in the absence of much longer waves or swell, the degree of saturation attained is defined by the balance of (2.9) and (2.10):

$$0.04 \cos\theta(u_*/c)^2 B = f(B). \quad (2.11)$$

The variation of the degree of saturation with wind stress (normalized by phase velocity) is then

$$\frac{\partial B}{\partial (u_*/c)^2} = 0.04 \cos\theta \left[\frac{\partial}{\partial B} \left(\frac{f(B)}{B} \right) \right]^{-1}. \quad (2.12)$$

According to the simplest ideas of a saturation spectrum independent of wind speed, the right-hand side of (2.12) would be zero since the slope of $f(B)$ is infinite at saturation. On the other hand, if a variation with wind speed of B as specified by (2.12) could be established reliably, then this would define the slope of the curve $f(B)$ near equilibrium.

Another constraint is provided by the observation that the local action density of these short waves on the ocean is stable to perturbations on a scale large compared with the wavelength, in the sense that if locally the action density is high, the increased spectral density of breaking reduces it, and if it is low, the decreased spectral density of breaking allows the wind input to restore the equilibrium. The larger, dominant wave components at large fetch and duration may show a "groupiness" as a result of the instabilities associated with nonlinear wave interactions, but as we have seen, the time scales of these instabilities at higher wavenumbers are negligibly slow compared with those of the wind input and wave breaking. If under a constant wind field, the degree of saturation B is perturbed by an amount B', then with the neglect of the resonant interactions, we have for the rate of change of the perturbation in action spectral density N',

$$\frac{\partial N'}{\partial t} = S_w(B + B') - D(B + B').$$

Since $N' = g^{1/2}k^{-9/2}B'$ and in the equilibrium state $S_w(B) = D(B)$, this can be expressed, using (2.9) and (2.10) as

$$\frac{1}{\sigma}\frac{\partial B'}{\partial t} = m(u_*/c)^2B' + [f(B) - f(B + B')], \quad (2.13)$$

where $m = 0.04\cos\theta$. For *small* perturbations B'

$$\frac{1}{\sigma}\frac{\partial B'}{\partial t} = \left\{m\left(\frac{u_*}{c}\right)^2 - \frac{\partial f}{\partial B}\right\}B',$$

and the condition for statistical stability is

$$\frac{\partial f}{\partial B} > m\left(\frac{u_*}{c}\right)^2, \quad (2.14)$$

which, in terms of Fig. 1, implies that the slope of the curve D as a function of B must be greater than that of S_w at the point of intersection (as, indeed, we had anticipated). As u_*/c increases, the equilibrium point rises and the slope df/dB at the equilibrium point increases even more rapidly. If the curve $f(B)$ can be expressed reasonably accurately as a power law, the relaxation rate

$$\gamma = \left\{\frac{\partial f}{\partial B} - m\left(\frac{u_*}{c}\right)^2\right\}\sigma \quad (2.15)$$

can be expressed simply and explicitly in terms of u_*/c. For, suppose that

$$f(B) = aB^n, \quad (2.16)$$

where n is certainly greater than one, then at equilibrium

$$m(u_*/c)^2B = aB^n,$$

so that

$$\frac{df}{dB} = naB^{n-1} = nm(u_*/c)^2,$$

$$\gamma = m(n - 1)(u_*/c)^2\sigma. \quad (2.17)$$

Even though the numerical value of n is not known (one might guess something in the range 3 to 5) this is a useful result. It can be written alternatively as

$$\gamma = m(n - 1)u_*^2g^{-2}\sigma^3, \quad (2.18)$$

showing that for a given wind stress, the relaxation rate towards equilibrium increases as the cube of the frequency for these short wave components.

However, if the perturbation in B is not small, the expected strong nonlinearity in $f(B)$ when B is small indicates that the recovery will be different for a local increase in degree of saturation from what it will be for a decrease. If the decrease in B is such that $f(B)$ is then negligible and breaking virtually ceases, the recovery will be initially at the undamped growth rate (proportional to the slope of the line in Fig. 1 marked S_w), which may be much slower than γ (proportional to the difference in the two slopes at the intersection.) A large local increase in B is then expected to disappear more rapidly by much enhanced breaking than a large local decrease in which breaking ceases. If at equilibrium between breaking and wind input (so that $S_w = D$) the degree of saturation is B_0, then from (2.9) and (2.10)

$$m(u_*/c)^2gk^{-4}B_0 = gk^{-4}aB_0^n,$$

when the representation (2.16) is used. Consequently

$$a = m(u_*/c)^2B_0^{1-n},$$

and the balance of the last two terms on the right-hand side of (2.6) can be written in terms of this equilibrium level as

$$gk^{-4}m(u_*/c)^2[1 - (B/B_0)^{n-1}]B. \quad (2.19)$$

3. The influence of a background sea state on mean short wave properties at given k

The short ocean wave components that are generally responsible for radar backscattering do not, of course, exist in isolation. Longer waves or swell produce modulations in the intensity of the backscattered return, measured by Wright *et al.* (1980) with a spatial scale of variation that images the long wave field. Beal (1981) has made use of these modulations to study the evolution and propagation of swell across the Atlantic continental shelf of the United States. Frequently, the orbital velocities associated with these longer waves are larger than the propagation speeds of the short components sensed and one's intuitive feeling might be that an irregular or random field of longer waves would so scramble the propagation

characteristics of the shorter waves as to obscure any likelihood of interpreting the large scale patterns in their intensity in terms of currents. However, this particular concern does not seem to be justified.

Consider a surface current field $\mathbf{U}(\mathbf{x}, t)$ whose scales of spatial and temporal variations L and T are large compared with the wavelength and period of long waves or swell, the scales over which the tangential components of their orbital velocity $\mathbf{u}$ varies. Local mean values of the wave field, indicated by an overbar, are defined over scales that are small compared with those of the current field but large compared with those of the swell. Fluctuations or modulations produced by the swell are represented by the difference between the actual values and the mean values defined in this way. Thus, the action density is represented as $\bar{N}(\mathbf{x}, t) + N'$, the short-wave group velocity at constant $\mathbf{k}$ (which varies because of the variations in the local g at the surface as the short waves ride over the swell) by $\bar{\mathbf{C}} + \mathbf{C}'$, and so forth. If the short waves are everywhere close to saturation under the balance of wind input and wave breaking, then (2.5) can be written as

$$\frac{\partial N}{\partial t} + (C_j + U_j + u_j)\frac{\partial N}{\partial x_j} - k_j \frac{\partial}{\partial x_j}(U_i + u_i)\frac{\partial N}{\partial k_i} = -\gamma(N - N_0), \quad (3.1)$$

where resonant wave–wave interactions are neglected, N_0 is the equilibrium value of N in the absence of long waves or currents and γ the relaxation rate of the previous section. Substitution of local mean and fluctuating quantities into (3.1) and averaging gives

$$\frac{\partial \bar{N}}{\partial t} + (\bar{C}_j + U_j)\frac{\partial \bar{N}}{\partial x_j} - k_j \frac{\partial U_i}{\partial x_j}\frac{\partial \bar{N}}{\partial k_i} = -\overline{(C_j' + u_j)\partial N'/\partial x_j} + k_j \overline{\frac{\partial u_i'}{\partial x_j}\frac{\partial N'}{\partial k_i}} - \gamma(\bar{N} - N_0). \quad (3.2)$$

The left-hand side of this equation has the same form as the original equation (2.6) so that the influence of the swell on the *mean* action spectral density is represented by the two new terms on the right. Now, to the first order, the wave-induced modulations N' are proportional to $\bar{N}$ (Wright *et al.* 1980) and to the root-mean-square slope ϵ of the long wave field, as are the local gradients with respect to $\mathbf{x}$ and $\mathbf{k}$, so that the covariance terms are of order $\epsilon^2\sigma_s\bar{N}$, where σ_s is the swell frequency. Their only effect, then, is to modify slightly (by order ϵ^2) the equilibrium mean spectral levels from those which would be obtained in the absence of swell.

The fact that the swell can therefore be ignored in a consideration of the local mean backscattering (over scales large compared with the swell wavelength) from short propagating waves is at first sight counter-intuitive, but the essence of the matter is that the modulation patterns at a *fixed wavenumber* are periodic and noncumulative provided the swell slope is sufficiently small that the dissipation response can be linearized.

4. Variations in N produced by surface currents

The dynamical balance (2.6) can be written in terms of the degree of saturation B by substituting $N = g^{1/2}k^{-9/2}B(k)$ and the expression (2.19).

$$\frac{\partial B}{\partial t} + (C_j + U_j)\frac{\partial B}{\partial x_j} + \frac{9}{2}\frac{k_i k_j}{k^2}\frac{\partial U_i}{\partial x_j}B - k_j \frac{\partial U_i}{\partial x_j}\frac{\partial B}{\partial k_i} = \sigma m\left(\frac{u_*}{c}\right)^2\left\{1 - \left(\frac{B}{B_0}\right)^{n-1}\right\}B. \quad (4.1)$$

If the magnitude of the current variations is represented by U_0 and the length scale over which they occur by L, then

$$\mathbf{U} = U_0\mathbf{f}(\mathbf{x}/L) = U_0\mathbf{f}(\boldsymbol{\xi}), \quad \text{say.}$$

Also, if $b(\boldsymbol{\xi}) = B/B_0$, the local degree of saturation relative to its equilibrium level, then under steady conditions (4.1) can be written in dimensionless form as

$$\left[\frac{C_j}{c} + \frac{U_0}{c}f_j(\boldsymbol{\xi})\right]\frac{\partial b}{\partial \xi_j} + \frac{9}{2}\frac{U_0}{c}\frac{k_i k_j}{k^2}\frac{\partial f_i}{\partial \xi_j}b - \frac{U_0}{c}k_j\frac{\partial f_i}{\partial \xi_j}\frac{\partial b}{\partial k_i} = \frac{mL\sigma}{c}\left(\frac{u_*}{c}\right)^2\{1 - b^{n-1}\}b = 2\pi m\left\{\frac{L}{\lambda}\left(\frac{u_*}{c}\right)^2\right\}\{1 - b^{n-1}\}b, \quad (4.2)$$

where c represents the phase velocity and λ the (fixed) wavelength of the components considered.

It is interesting to note that this equation involves only two basic parameters, U_0/c expressing the strength of the current field and $S = (L/\lambda)(u_*/c)^2$ representing the combined influence of the wind, the scale of the current field and, implicitly, breaking. This second parameter can also be written as

$$2\pi\frac{Lu_*^2}{\lambda^2 g}, \quad \text{or as} \quad \frac{1}{2m}\left(\frac{L}{C}\right)\left\{m\sigma\left(\frac{u_*}{c}\right)^2\right\},$$

where C is the group velocity. The latter form provides a useful physical interpretation of this parameter as proportional to the ratio of the time taken for an energy packet to move over one scale distance L to the characteristic growth time of the waves under the influence of the wind alone. If this parameter is large, readjustment of the waves is rapid in the time taken to traverse the current variation, so that the response in the relative degree of saturation is small. Small

values of the parameter indicate situations where the readjustment time is long, so that one might expect a significant response.

For the sake of definiteness, suppose that the 1-direction in (4.2) is chosen as the direction of the wavenumber being sampled. The middle term on the left-hand side then reduces to

$$\frac{9}{2}\frac{U_0}{c}\frac{\partial f_1}{\partial \xi_1} b,$$

expressing the influence of convergence or divergence of the current field in this direction. The third term involves the variation with respect to magnitude and direction of the degree of saturation and must be considered when a current, varying in x, is in the transverse direction so that energy paths are deflected. Little is known (although much is speculated) about the angular distribution of the wave spectrum or b, so that in order to obtain a sense of the magnitude to be expected of the variations in the local degree of saturation relative to the background, we will neglect the variations of b with k and consider convergences or divergences only with $U_1 = U(x_1)$. In the flow over relatively shallow topography such as the Nantucket Shoals, both local convergences ($\partial U/\partial x < 0$) and divergences ($\partial U/\partial x > 0$) can be expected; under open sea conditions, divergences would be expected in regions of local upwelling while local convergences may be found along fronts, with one water mass overriding another, slightly denser.

With $\mathbf{f}(\xi) = (f(\xi), 0, 0)$, say, Eq. (4.2) reduces to

$$\left(\frac{1}{2} + \frac{U_0}{c} f(S)\right)\frac{db}{d\xi} + \frac{9}{2}\frac{U_0}{c}\frac{df}{d\xi} b = 2\pi m S(1 - b^{n-1})b, \tag{4.3}$$

where S is the sensing parameter $(L/\lambda)(u_*/c)^2$. The value of the index n, although greater than 1, is not known at this time; for the purposes of these calculations n was taken as 3. A smaller value gives a more gradual onset of energy loss by breaking as b increases and so a larger response to convergences; a larger value reduces the response. This is shown explicitly as follows. The wind is supposed to act in the x-direction also so that $m = 0.04$ and a current distribution of the form

$$f(\xi) = \tfrac{1}{2}\{1 + \tanh\xi\}$$

was chosen. The Eq. (4.3) was integrated numerically with $b = 1$ at $\xi = -2$ for various values of U_0/c and S, using an Apple II computer. When $U_0/c < -0.5$, Eq. (4.3) has a mathematical singularity at which the coefficient of the first turn vanishes. In those cases, the integrations were performed following the direction of the wave energy flow, from $\xi = -2$ to within one step of the singularity and then from $\xi = +6$ back to the singularity since in this part of the physical domain, the backwards energy convection of the current overcomes the forwards propagation. If the waves on the far side of the convergence zone have had sufficient fetch and duration to achieve equilibrium, then $b = 1$ at $\xi = 6$ also and it is found, somewhat surprisingly, that the two branches of the solution form a continuous curve across the singularity at which $[1/2 + (U_0/c) f(\xi)] = 0$. On the other hand, if the fetch or duration on the far side is limited, then b on the far side may be less than unity for these waves and a real, physical singularity will occur at this point. It seems that only in this case will an abrupt change in the return signal coincide with this singularity.

Some results of these calculations are illustrated in Fig. 2. When the parameter S is O ($\geqslant 10$), the responses of b to the current field are small and limited essentially to the region of current variation. For smaller values of S, the magnitude of the response increases; in a convergence ($U_0/c < 0$) the region over which b is significantly greater than 1 remains limited to the convergence region because of the relatively rapid reduction in wave energy by breaking. However, in a divergence the degree of saturation at a given k reduces as a result of two effects—the divergence spreads the action density out over a greater spatial interval and (more important) the energy packet at the wavenumber observed after divergence was, before the divergence, at a larger wavenumber or smaller scale, so that its action density was less. At values of S less than about 4, the recovery distance of the wave field after suppression is significantly greater than L so that the waves remain unsaturated for a considerable distance.

In a convergence zone, the maximum degree of saturation relative to the background occurs close to the point of maximum strain rate, when $f'(\xi) = 1$. From (4.3) this occurs when

$$-\frac{9}{2}\frac{U_0}{c} = 2\pi m S(1 - b^{n-1})$$

so that the maximum contrast is

$$b_{\max} = \left\{1 + \frac{9}{4\pi m}\frac{U_0}{cS}\right\}^{1/(n-1)}. \tag{4.4}$$

In the cases shown in Fig. 2, n has been taken as 3; since the coefficient $\frac{9}{4}\pi m \approx 20$, $b_{\max}$ varies approximately as $(U_0/c)^{1/2}S^{-1/2}$ for values of $S < 4U_0/c$ or so. But the value of the index n in the representation (2.15) cannot be regarded as known and, in fact, the expression (4.4) may allow it to be determined by field measurements of the maximum contrast in the degree of saturation at a fixed k in convergence zones over a range of values of S and U_0/c, although if n is significantly greater than 1 (as expected), the dependence on n is rather weak.

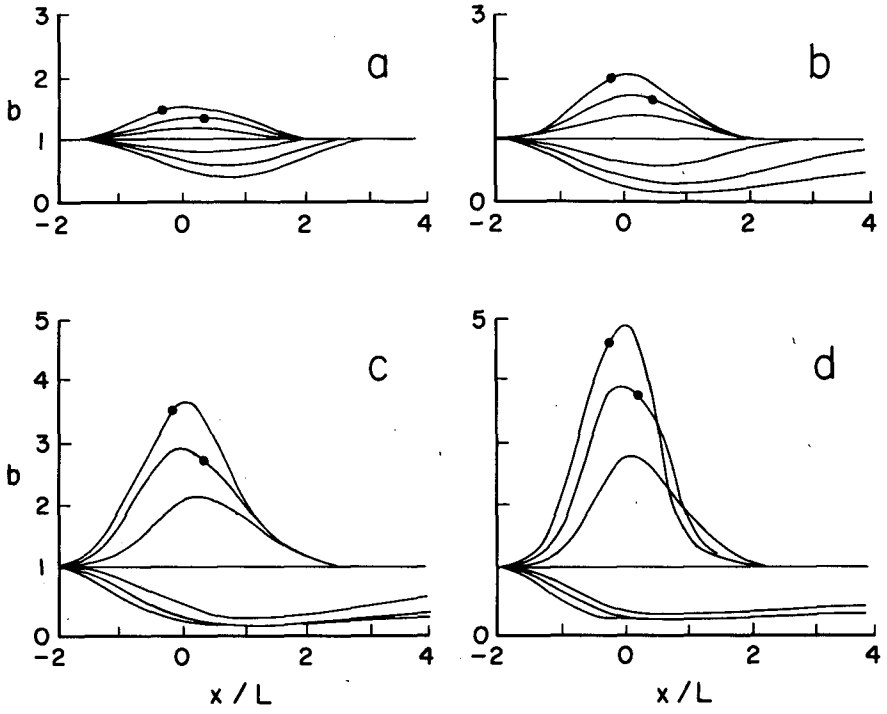

FIG. 2. Relative degrees of saturation $b = B/B_0$ at a fixed wavenumber as functions of position in a local convergence or divergence centered at $x = 0$: in (a) $S = (L/\lambda)(u_*/c)^2 = 12$; in (b) 4; in (c) 1 and in (d) 0.5. The three upper curves in each group represent the convergence cases with $U_0/c = -1.2$, -0.8 and -0.4; the three lower curves are for divergences with $U_0/c = 0.4$, 0.8 and 1.2. The black dots represent positions where $U(x)/c = -0.5$.

A general conclusion from these computations is that if freely propagating waves under the influence of wind and breaking are to experience a significant variation in the degree of saturation at a fixed wavelength λ, then the second term in the bracket of (4.4) must be greater than unity, say, or

$$\frac{U_0}{cS} \gtrsim 0.05. \tag{4.5}$$

Expressed alternatively in terms of the strain rate in a convergence, a significant response requires

$$\frac{U_0}{L} \gtrsim 0.12 \frac{u_*^2}{g^{1/2}\lambda^{3/2}}. \tag{4.6}$$

For example, if $u_* = 20$ cm s^{-1} and $\lambda = 16$ cm, then U_0/L must be greater than about 2×10^{-2} s^{-1}, which is a very large oceanic strain rate outside frontal regions. Light winds clearly favour a more sensitive response.

It should be noted, however, that for a given convergence field and wind stress, (4.4) can be written as

$$b_{\max} = \left\{1 + \frac{9}{2} m^{-1}(2\pi)^{-3/2} \frac{U_0 g^{1/2}\lambda^{3/2}}{L\mu_*^2}\right\}^{1/(n-1)}, \tag{4.7}$$

and the contrast in degree of saturation increases with wavelength, the smaller value of U_0/c being more than compensated by the increase in S^{-1}. Increased harmonic content of these longer waves and denser breaking patches may give enhanced Bragg and specular scattering that may possibly dominate the direct return from freely travelling waves at the wavenumber sensed by Bragg scattering in the background.

In a region of surface divergence (and upwelling), when S is small the recovery of the wave field by the wind is slow over the scale of the divergence, and the reduction in b can be estimated by neglecting the wind input (and wave breaking) over this interval. With $U_0 f(\xi) = U(\xi)$, Eq. (4.3) reduces to

$$\left(\frac{1}{2} + \frac{U(\xi)}{c}\right)\frac{db}{d\xi} + \frac{9}{2}\frac{d}{d\xi}\left(\frac{U(\xi)}{c}\right)b = 0,$$

which integrates exactly to

$$b(\xi) = (1 + 2U(\xi)/c)^{-9/2}, \tag{4.8}$$

since $b = 1$ when $U = 0$. This reduction $[U(\xi) > 0]$ at a fixed wavenumber is, of course, greater than for an energy packet or wave train at a fixed apparent frequency, as calculated by Longuet-Higgins and Stewart (1960) since the waves elongated by the divergence to the wavenumber k had a larger wavenumber and smaller spectral density than the waves at wavenumber k before the straining.

The Seasat synthetic aperture radar imagery, such as that reproduced in the book by Beal *et al.* (1981; see especially p. 22 and 96), offers a number of examples that seem, in the light of these results, to be interpretable as lines of local convergence or divergence. There is unfortunately little independent information on the current field or the local wind stress so that attempts at a quantitative comparison must await imagery for which more complete documentation, particularly "ground truth" measurements of the surface current variations, become available. Nevertheless, the analysis given here does allow the following conclusions to be drawn:

1) The magnitude of the response of short gravity waves to variations in surface current is, from (4.4) and (4.5), a function of the combination

$$\frac{U_0}{cS} = \frac{U_0}{L}\frac{2\pi c^3}{gu_*^2}$$

rather than of the strain rate or of U_*/c separately; for strain rates characteristic of oceanic conditions, the response is small except under light wind conditions.

2) The patterns produced by local convergences and divergences are characteristically different; in a local convergence the augmentation in degree of saturation is limited to the convergence zone and recovers rapidly beyond it, while in a divergence, the reduction occurs in the divergence zone and recovery to the equilibrium level is more gradual.

3) These conclusions are insensitive to the precise parameterization of the rate of energy loss in terms of the degree of saturation. Nevertheless, measurements in a strong convergence such as those produced by tidal flows over relatively shallow bottom topography should allow, through (4.4), estimates of the index n which is at present unknown.

Acknowledgments. It is a pleasure to acknowledge the support of NASA during the early stages of this investigation under Contract NAGW-304. It was completed with the support of the Fluid Dynamics Branch of the Office of Naval Research under Contract N00014-76-C-0184.

REFERENCES

Banner, M. L., 1984: A comparison of the wave-induced momentum flux to breaking and non-breaking waves. *Wave Dynamics and Radio Probing of the Ocean Surface.* K. Hasselmann and O. M. Phillips, Eds., Plenum Press.

——, and W. K. Melville, 1976: On the separation of air flow over water waves. *J. Fluid Mech.*, **77**, 825–842.

Beal, R. C., 1981: Spatial evolution of ocean wave spectra. *Spacebourne Synthetic Aperture Radar for Oceanography*, 110–127.

——, P. S. DeLeonibus and I. Katz, Eds., 1981: *Spacebourne Synthetic Aperture Radar for Oceanography.* The Johns Hopkins University Press, 215 pp.

Fox, M. J. H., 1976: On the nonlinear transfer of energy in the peak of a gravity wave spectrum, II. *Proc. Roy. Soc. London*, **A348**, 467–483.

Gent, P. R., and P. A. Taylor, 1976: A numerical model of the air flow above water waves. *J. Fluid Mech.*, **77**, 105–128.

Keller, W. C., and J. W. Wright, 1975: Microwave scattering and the straining of wind-generated waves. *Radio Sci.*, **10**, 139–147.

Kitaigorodskii, S. A., 1983: On the theory of the equilibrium range in the spectrum of wind-generated gravity waves. *J. Phys. Oceanogr.*, **13**, 816–827.

Longuet-Higgins, M. S., and R. W. Stewart, 1960: Changes in the form of short gravity waves on long waves and tidal currents. *J. Fluid Mech.*, **8**, 565–583.

Mitsuyasu, H., and T. Honda, 1984: The effects of surfactant on certain air–sea interaction phenomena. *Wave Dynamics and Radio Probing of the Ocean Surface*, K. Hasselmann and O. M. Phillips, Eds., Plenum Press.

Phillips, O. M., 1958: The equilibrium range in the spectra of wind-generated waves. *J. Fluid Mech.*, **4**, 426–434.

——, 1980: *The Dynamics of the Upper Ocean, 2nd ed.* Cambridge University Press, 336 pp.

——, and M. L. Banner, 1974: Wave breaking in the presence of wind drift and swell. *J. Fluid Mech.*, **66**, 625–640.

Plant, W. J., 1982: A relationship between wind stress and wave slope. *J. Geophys. Res.*, **87**, 1961–1967.

Toba, Y., and H. Kunishi, 1970: Breaking of wind waves and the sea surface wind stress. *J. Oceanogr. Soc. Japan*, **26**, 71–80.

West, B. J., 1984: Statistical properties of water waves, Part IV. *Wave Dynamics and Radio Probing of the Ocean Surface*, K. Hasselmann and O. M. Phillips, Eds., Plenum Press.

Wright, J. W., W. J. Plant, W. C. Keller and W. L. Jones, 1980: Ocean wave-radar modulation transfer function from the West Coast experiment. *J. Geophys. Res.*, **85**, 4957–4966.